

Observation of electronic and atomic shell effects in gold nanowires

A. I. Mares, A. F. Otte, L. G. Soukiassian, R. H. M. Smit, and J. M. van Ruitenbeek
Kamerlingh Onnes Laboratorium, Universiteit Leiden, Postbus 9504, NL-2300 RA Leiden, The Netherlands
 (Received 26 April 2004; published 20 August 2004)

The formation of gold nanowires in vacuum at room temperature reveals a periodic spectrum of exceptionally stable diameters. This is identified as shell structure similar to that which was recently discovered for alkali metals at low temperatures. The gold nanowires present two competing “magic” series of stable diameters, one governed by electronic structure and the other by the atomic packing.

DOI: 10.1103/PhysRevB.70.073401

PACS number(s): 73.40.Jn, 61.46.+w, 68.65.La

When the conductance of metallic nanowires can be described in terms of a finite number of quantum modes it is expected that the degree of filling of the quantum modes has a measurable effect on the total free energy of the nanowires.^{1–3} Indeed, Yanson *et al.*⁴ observed that alkali nanowires, obtained by the mechanically controllable break junction (MCBJ) technique, exhibit exceptional stability for certain diameters. The series of stable diameters was shown to correspond directly to the well-known magic number series of alkali metal clusters produced in vapor jets (for a review see Ref. 5). For alkali metal clusters and nanowires the main features of this electronic shell effect can be understood in terms of the filling of simple free-electron modes inside a spherical or cylindrical cavity, respectively. The electronic level spectrum shows groups of levels bunched together and a cluster or nanowire is favored when such a shell is just filled. The principle of this shell structure is well known from atomic physics, giving rise to the periodic table of the elements, and from nuclear physics, explaining the periodic appearance of stable nuclei. Apart from this electronic shell structure alkali metal clusters and nanowires show, typically at larger diameters, a second series of stable diameters resulting from the atomic structure. Completed atomic layers stabilize the nanowires.

The alkali nanowires are very attractive from a fundamental point of view, since the electronic structure is well described in terms of free and independent electrons, but they are not very suitable for possible applications. As suggested by research on metal clusters shell effects for nanowires should be observable for many other metals. As a first step beyond the alkali metals we have chosen gold, since the physics is expected to be very similar, it being to a good approximation still a free-electron metal.

Recently some experimental results on the formation and stability of gold nanowires have already been reported. By the use of an electron beam thinning technique in a transmission electron microscope under ultra-high vacuum at $T = 300$ K Kondo and Takayanagi⁶ observed gold nanowires that adopt a series of unusual helical configurations, which is an exceptional form of atomic shell structure. Using STM indentation experiments Medina *et al.*^{7,8} reported the observation of atomic shell effects in gold nanowires. Here, we demonstrate clear evidence for *electronic* shell effects, with a crossover to atomic shell structure at larger diameters.

The atoms need to have sufficient mobility in order to be able to explore many wire configurations and find the stable

ones corresponding to shell filling. Therefore, in order to observe shell effects we need to raise the temperature to a sizeable fraction of the bulk melting temperature. For the alkali metals a temperature near 80 K was sufficient and the experiments were performed with a standard low-temperature MCBJ device with a local heating extension.⁴ For gold this is not sufficient and we have developed a new MCBJ instrument (Fig. 1) operating under ultra high vacuum (UHV) allowing the temperature to be varied between 70 and 500 K. A notched gold wire is fixed with stainless steel clamps, bridging two bendable metal substrates. The wire is broken at the notch in a controlled way by mechanically applying pressure from below onto both substrates. Once broken the bending beams can be relaxed to bring the wire ends back into contact and atomic-sized contacts can be finely adjusted using a piezoelectric element. The base pressure is 5×10^{-10} mbar.

Nanowires are obtained by indenting the two clean fracture surfaces and subsequently stretching the contact while monitoring the conductance of the wire. The conductance trace follows a sequence of plateaus separated by abrupt jumps. At the final stages the contact consists of just a few atoms and the conductance is changing in steps signaling the atomic structural rearrangements of the contact. For monovalent metals the conductance of a single-atom contact is close to $1 G_0 = 2e^2/h$, and carried by a single conductance channel.⁹ The conductance is measured at constant bias voltage, recording the current through a current-voltage conver-

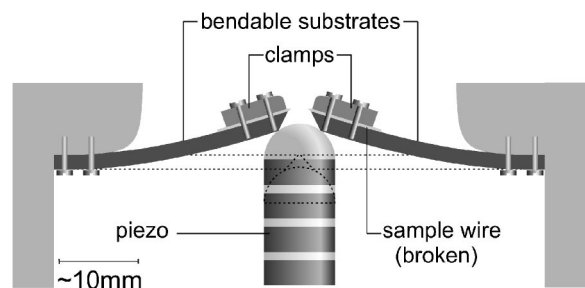


FIG. 1. Schematic view of the MCBJ technique under UHV. The sample wire is clamped onto two separate bending beams, having a notch at the bridging point, and broken by bending the beams. Contact between the fracture surfaces can be finely adjusted by means of the piezoelectric element. The relaxed configuration of the sample is represented by the dotted lines.

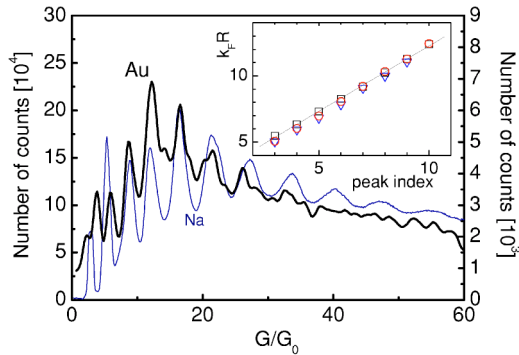


FIG. 2. (Color online) Conductance histogram for gold (bold curve, right axis) giving evidence for electronic shell structure. It is obtained at room temperature from 2000 individual consecutive traces, using a bin-size of $\sim 0.1 G_0$ and a bias voltage of 300 mV. For comparison similar data from Ref. 4 obtained for Na at 80 K are shown (thin curve, left axis). The inset shows the peak positions, converted to $k_F R$, as a function of peak index for three independent experiments on Au.

tor and a 16 bit analog-to-digital converter. A trace from $100 G_0$ to 0 is recorded in about 10 s at a sampling rate of 10 ms.

At larger diameters the conductance jumps can be larger and each conductance trace is different depending on the evolution of atomic arrangements in the nanowire. In order to reveal underlying variations in stability we perform a simple statistical analysis by adding all values of the digitized conductance traces into conductance histograms. Preferred nanowire structures are then seen as maxima in the conductance histograms. The wire radius R corresponding to a given conductance value can be obtained from a semiclassical expression^{10,11}

$$G \cong G_0 \left[\left(\frac{k_F R}{2} \right)^2 - \frac{k_F R}{2} + \frac{1}{6} \right], \quad (1)$$

with k_F the Fermi wave vector.

Figure 2 shows a conductance histogram up to a conductance of $60 G_0$ obtained for gold at room temperature (bold curve). The histogram is five-point smoothed by using a second order polynomial. The data show strong resemblance to the histogram for Na recorded at $T=80$ K by Yanson *et al.*,⁴ which is shown for comparison in the same graph. The high counts at the peaks result from stable wire diameters. The peaks between 7 and $25 G_0$ agree very well. Above $25 G_0$ only one or two more peaks are visible for Au, much less than for Na, and they may be shifted somewhat to lower conductance. The first few peaks below $7 G_0$ do not correspond very well. The low-conductance histograms for Na have been shown before to differ significantly from those for Au.^{12,13} The direct correspondence in period and phase of the two series of peaks at higher G is strong evidence for similar electronic shell structure in Au and Na.

For shell effects the peaks are expected to be equidistant when plotted as a function of the radius of the wire. This is verified in the inset to Fig. 2, where we plot $k_F R$ obtained from Eq. (1) as a function of peak index. The peaks have

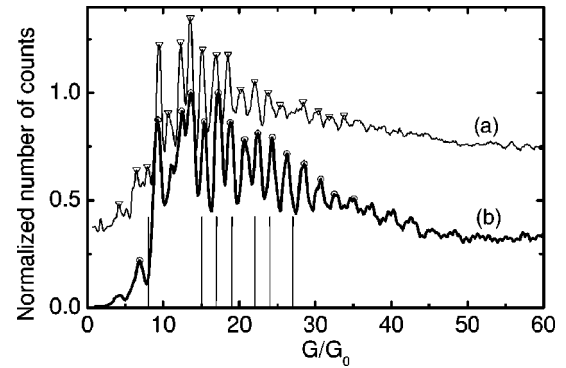


FIG. 3. Second type of conductance histogram for Au at room temperature, giving evidence of electronic and atomic shell effects with a crossover at $G \approx 12 G_0$. (a) Obtained from 3000 individual conductance traces recorded at a bias voltage of 150 mV. (b) Recorded at 100 mV, combining 5000 traces, evidencing mainly atomic shell effect, since only the first two peaks can be related to electronic shell effect. For comparison the positions of the stable helical gold nanowires proposed by Kondo *et al.* (Ref. 6) are marked by vertical lines.

been reproduced for different samples in six independent series of measurements on Au and in order to illustrate the degree of reproducibility the plot contains points from three measurements. The period $\Delta k_F R$ shows some variation between the individual measurements that averages as $\Delta k_F R = 1.02 \pm 0.04$. This is somewhat smaller than the slopes for electronic shell structure observed for the alkali metals.¹⁴

Often we observe another periodic structure in gold conductance histograms recorded under similar experimental conditions, as illustrated by two examples in the Fig. 3. Many histograms show a crossover between the electronic shell period of Fig. 2 to a new shorter period. The peaks were identified using a software tool (symbols) and Fig. 4 shows the radii corresponding to the peaks in Fig. 3(a). The crossover is at the second point, above which we find a period

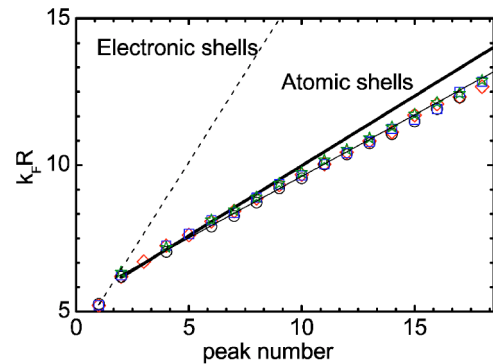


FIG. 4. (Color online) Positions of the peaks in the histograms for four independent experiments, including those from Fig. 3, reproducibly showing evidence for a second set of periodic stable diameters. The dashed line gives the expected slope for electronic shell structure; the bold line gives the slope for the stable radii of atomic shells expected from close packing of the nanowire along the [110] axis, $\Delta k_F R = 0.47$. In the experiment the slope above the second point is $\Delta k_F R = 0.4 \pm 0.01$. This is somewhat smaller (see text) but suggests an explanation in terms of atomic shell structure.

$\Delta k_F R = 0.40 \pm 0.01$. This structure has been reproduced in well over ten independent measurements and a second example is shown in Fig. 3(b) for comparison. It can be seen that the period $\Delta k_F R$ displays some variation, giving an overall average of $\Delta k_F R = 0.40 \pm 0.03$. Again, this second periodic structure agrees closely to the results obtained for alkali nanowires and by analogy we interpret it as an *atomic* shell effect.

Thus we attribute the peaks in the histograms in Figs. 2 and 3 to two different and independent effects: electronic and atomic shell effects. The electronic shell effect gives rise to peaks in the histograms because specific radii of the nanowire are more stable than average due to local minima of the electronic energy of the system. Electronic shell effects have been previously found for clusters of gold atoms in vapor jets.¹⁵ The magic number series of stable clusters has been successfully explained by approximating the electronic structure of gold metal by homogeneous free-electron (jellium) models^{5,16} confined by a spherically symmetric potential well. In the same spirit we model our nanowires as a free electron gas confined by a cylindrical potential well.^{2,3,11,17} The magic diameters are obtained by a semiclassical approach using the Bohr-Sommerfeld quantization condition. Stable trajectories for the electron wave packets are periodic orbits inside a cylinder, that can be classified as diametric, triangular, square, etc. Each of these trajectories gives rise to a periodic series of oscillations in the density of states as a function of $k_F R$, that produce oscillations in the total energy of the system. The dominant period of the oscillation depends somewhat on the electron density and the shape of the potential well. We obtain a number of $\Delta k_F R = 1.21 \pm 0.02$ using an electron density corresponding to that for gold from the calculations by Ogando *et al.*,¹⁷ which agrees well with the periodicity of shell structure in gold clusters, $\Delta k_F R = 1.23 \pm 0.01$. The differences in the peaks observed for Na and Au at low G can be largely explained by considering elliptically distorted wires and including differences in surface tension for the two metals.¹⁸ However, we find a reproducible peak at $4 G_0$ for gold, which does not appear in this analysis and may be due to quadrupolar distortions (see Ref. 18).

The period obtained experimentally for gold nanowire magic radii, $\Delta k_F R = 1.02 \pm 0.04$, is slightly smaller than that expected from the semiclassical analysis. Deviations similar to the present results for Au have been observed for Li.¹⁴ Such deviations have been attributed to backscattering of the electrons on defects, which is not included in the idealized semiclassical model. Defect scattering may also explain the observed variation of the slopes between experiments and the fact that the range of observed oscillations for Au is smaller than for Na, since scattering will lead to smearing of the peaks. In order to preserve a constant slope the correction should be proportional to the conductance G itself. In other words, a certain fraction of the electrons is scattered back, independent of the wire radius. This would for instance be the case when the dominant mechanism is scattering by roughness on the nanowire surface, which seems plausible.

The Fermi surface of bulk gold has marked deviations from spherical symmetry. The nearly spherical main sheets of Fermi surface are connected by necks across the Brillouin

zone boundaries. The necks may introduce an additional set of oscillations in the density of states. However, since the wavelength of the states in the neck is about six times larger than the main Fermi wavelength the period would be much larger than that due to the main states. Moreover, the number of states in the neck is small making the amplitude of the effect small. Thus we expect that it is a good approximation to consider gold as free electron metal having the same electronic shell effect as in alkali metals. This is supported by electronic structure calculations¹⁹ for the quantum modes in nanowires of Na and Cu (which has a Fermi surface similar to Au).

For larger radius R the configuration energy (atomic shell structure) becomes more important than the energy contribution due to the conduction electrons. The amplitude of the oscillations in the electronic free energy scales as $1/R$,²⁰ while the ones for the surface energy increase proportional to R , making the latter dominant at large radii. The crossover point is seen to vary between experiments, which is likely due to differences in the local crystal orientation of the leads connecting the nanowire. Note that the histogram in Fig. 2 shows some additional fine structure that may be due to an admixture of atomic shell structure.

The [110] orientation has been shown to be most favorable to form nicely faceted long nanowires.^{21,22} At large diameters we expect the nanowires to order into densely packed wires, that minimize the surface energy. We assume that the bulk fcc packing of gold is preserved, which is supported by the observation of gold nanowires in transmission electron microscopy by Rodrigues *et al.*²¹ The lowest energy surfaces for gold are perpendicular to [111] and we can construct a densely packed wire along a [110] axis with four (111) and two (100) facets, as also proposed by Ref. 22. Completing a full atomic shell gives rise to a rather long period of $\Delta k_F R = 2.85$, but assuming stable wires are found when completing a single facet we obtain a six times smaller period $\Delta k_F R = 0.476$.²³ The faceting structure of stable wires can be recognized in a Monte Carlo simulation of the thinning down of a fcc wire by Jagla and Tosatti.²² The experimental slope is about 20% smaller than expected, but this is consistent with a similar deviation observed for the electronic shell effect and is similarly attributed to defect scattering.

Our results and interpretation differ in several essential points from the work in Ref. 8, where the observed structure is entirely attributed to atomic shell structure. However, the well-developed peak numbers 3, 4, and 5 in Fig. 1 of Ref. 8 agree with the first three peaks of what we interpret as electronic shell structure in Fig. 2. We have no need to resort to a second-derivative analysis, as was done in the cited work to analyze the histograms at higher G , which entails the risk of identifying residual fluctuations in the background as peaks. Also, our peak structure shows the expected global decrease of the amplitude towards larger diameters, in contrast to the data by Medina *et al.*^{7,8} We conclude that electronic shell structure is clearly observed in Au nanowires, with a crossover to atomic shells at larger diameters.

Apart from atomic shell structure based on conventional fcc lattice packing one should consider the “weird wire” configurations that have been predicted²⁴ and observed for gold

in transmission electron microscopy.⁶ The helical atomic wire arrangements lead to a series of “shells” for which we estimate the conductances shown by bars in Fig. 3. In view of the much more regular pattern observed we conclude that under conditions used in our experiment the regular lattice atomic shell structure is predominant. This may be a consequence of the path by which the nanowire evolves from a large fcc wire down. Making a structural crossover to helical

arrangement along the way presumably involves a relatively large barrier.

We thank R. van Egmond for valuable assistance with the experiments, and J. Bürki, H. Grabert, and D. Urban for discussions. This work is part of the research program of the “Stichting FOM,” and was supported by the EU TMR Network program DIENOW.

-
- ¹J. M. van Ruitenbeek, M. H. Devoret, D. Esteve, and C. Urbina, *Phys. Rev. B* **56**, 12 566 (1997).
- ²C. A. Stafford, D. Baeriswyl, and J. Bürki, *Phys. Rev. Lett.* **79**, 2863 (1997).
- ³C. Yannouleas and U. Landman, *J. Phys. Chem. B* **101**, 5780 (1997).
- ⁴A. I. Yanson, I. K. Yanson, and J. M. van Ruitenbeek, *Nature (London)* **400**, 144 (1999).
- ⁵W. A. de Heer, *Rev. Mod. Phys.* **65**, 611 (1993).
- ⁶Y. Kondo and K. Takayanagi, *Science* **289**, 606 (2000).
- ⁷E. Medina, M. Díaz, N. León, C. Guerrero, A. Hasmy, P. A. Serena, and J. L. Costa-Krämer, *Phys. Rev. Lett.* **91**, 026802 (2003).
- ⁸M. Díaz, J. L. Costa-Krämer, E. Medina, A. Hasmy, and P. A. Serena, *Nanotechnology* **14**, 113 (2003).
- ⁹E. Scheer, N. Agrait, J. C. Cuevas, A. Levy Yeyati, B. Ludoph, A. Martín-Rodero, G. Rubio Bollinger, J. M. van Ruitenbeek, and C. Urbina, *Nature (London)* **394**, 154 (1998).
- ¹⁰J. A. Torres, J. I. Pascual, and J. J. Sáenz, *Phys. Rev. B* **49**, 16 581 (1994).
- ¹¹C. Höppler and W. Zwerger, *Phys. Rev. Lett.* **80**, 1792 (1998).
- ¹²M. Brandbyge, J. Schiøtz, M. R. Sørensen, P. Stoltze, K. W. Jacobsen, J. K. Nørskov, L. Olesen, E. Lægsgaard, I. Stensgaard, and F. Besenbacher, *Phys. Rev. B* **52**, 8499 (1995).
- ¹³J. M. Krans, J. M. van Ruitenbeek, V. V. Fisun, I. K. Yanson, and L. J. de Jongh, *Nature (London)* **375**, 767 (1995).
- ¹⁴A. I. Yanson, Ph.D. thesis, Universiteit Leiden, The Netherlands (2001).
- ¹⁵I. Katakuse, T. Ichihara, Y. Fujita, T. Matsuo, T. Sakurai, and H. Matsuda, *Int. J. Mass Spectrom. Ion Processes* **67**, 229 (1985).
- ¹⁶M. Brack, *Rev. Mod. Phys.* **65**, 677 (1993).
- ¹⁷E. Ogando, N. Zabala, and M. J. Puska, *Nanotechnology* **13**, 363 (2002).
- ¹⁸D. F. Urban, J. Bürki, C.-H. Zhang, C. A. Stafford, and H. Grabert, cond-mat/0312517 (unpublished); private communication.
- ¹⁹J. Opitz, P. Zahn, and I. Mertig, *Phys. Rev. B* **66**, 245417 (2002).
- ²⁰C. Yannouleas, E. N. Bogachek, and U. Landman, *Phys. Rev. B* **57**, 4872 (1998).
- ²¹V. Rodrigues, T. Fuhrer, and D. Ugarte, *Phys. Rev. Lett.* **85**, 4124 (2000).
- ²²E. A. Jagla and E. Tosatti, *Phys. Rev. B* **64**, 205412 (2001).
- ²³A. I. Yanson, I. K. Yanson, and J. M. van Ruitenbeek, *Phys. Rev. Lett.* **87**, 216805 (2001).
- ²⁴O. Gülseren, F. Ercolessi, and E. Tosatti, *Phys. Rev. Lett.* **80**, 3775 (1998).